Gravitational wave as a probe of light feebly interacting dark matter

Yuchao Gu,[1,2,*] Liangliang Su,[1,†] Lei Wu,[1,‡] Yongcheng Wu,[1,§] and Bin Zhu[3,‖]
[1]*Department of Physics and Institute of Theoretical Physics, Nanjing Normal University, Nanjing 210023, China*
[2]*Key Laboratory of Dark Matter and Space Astronomy, Purple Mountain Observatory, Chinese Academy of Sciences, Nanjing 210023, China*
[3]*Department of Physics, Yantai University, Yantai 264005, China*

(Received 17 December 2023; accepted 2 June 2024; published 19 July 2024)

Light feebly interacting dark matter is widely predicted in a plethora of new physics models. However, due to very feeble couplings with the standard-model particles, its relic density produced via the relativistic thermal freeze-out process easily exceeds the observed value. The entropy dilution in an early matter-dominated era provides an attractive mechanism for solving such an overabundance problem. In this work, we note that this dark matter dilution mechanism will lead to two distinctive kinks in the primordial GW spectrum, whose frequencies strongly correlate with the DM mass. We show that the GW detectors, such as Cosmic Explorer (CE) and Big Bang Observer (BBO), can measure the kinks in the primordial GW spectrum and will offer a new avenue to probe light feebly interacting dark matter.

DOI: 10.1103/PhysRevD.110.015022

I. INTRODUCTION

The weakly interacting massive particle (WIMP) has long been considered a compelling candidate for DM and has been extensively searched for in collider, direct, and indirect detection experiments [1–12]. However, despite these efforts, no unambiguous signal confirming the existence of WIMPs has been observed. Conversely, these experimental observations have imposed stringent limits on the parameter space of WIMPs [13,14]. Consequently, light feebly interacting DM candidates, such as the gravitino and axino [15–19], have gained significant attention due to their ability to evade the constraints from direct-detection experiments, where their superweak coupling to visible particles makes them unlikely to be probed through conventional direct-detection searches. However, the light feebly interacting DM can be probed at the colliders [20,21], but also through using telescopes and neutrino experiments to detect the decay products of parent particles [22–25]. Furthermore, the primordial gravitational waves (GWs) can be regarded as a probe that detects high-energy physics from the end of inflation to big bang nucleosynthesis. The primordial GWs therefore can be utilized to probe such light feebly interacting DM.

During the early high-temperature phase of the Universe, light feebly interacting DM would have been brought into thermal equilibrium with the surrounding particles. As a result, the relic density of such DM, produced through thermal production mechanisms [26–30], could potentially lead to an overclosure of the Universe due to its small annihilation rate compared to WIMP DM [31,32]. Intriguingly, the overproduced abundance of DM can be diluted by the additional production of entropy, aligning it with the observed value. This additional entropy production can be generated by the late decays of certain states [20,25,33–42], which often give rise to an early matter-dominated era (EMD), preceding the regular radiation-dominated epoch.

Furthermore, the recent milestone discovery of gravitational waves has opened up a new era in astronomy and cosmology [43–45]. GWs induced by cosmic strings [46–48], primordial inflation [49], and strong first-order phase transition [50,51] offer novel cosmological probes that provide an exciting opportunity to investigate the early Universe's history [52–69], including an EMD era. The EMD era can modify the GW spectrum, thus offering the potential to search for light feebly interacting DM through the detection of GW signals.

In this paper, we investigate the role of inflationary GWs as a probe for light feebly interacting DM. Notably, the EMD era induces distinctive features in the primordial GW spectrum where there exist two kinks. The frequencies of

*Contact author: guyc@njnu.edu.cn
†Contact author: liangliangsu@njnu.edu.cn
‡Contact author: leiwu@njnu.edu.cn
§Contact author: ycwu@njnu.edu.cn
‖Contact author: zhubin@mail.nankai.edu.cn

these kinks are determined by parameters associated with the EMD epoch. Additionally, these parameters govern the magnitude of the dilution effect occurring during the EMD era and are connected to the mass of the DM candidate through the overproduced DM abundance. Consequently, the EMD era serves as a bridge between GWs and DM, providing a unique opportunity to probe light feebly interacting DM across different mass ranges using inflationary GW observations. By exploring the relationship between the EMD era, the primordial GW spectrum, and the properties of light feebly interacting DM, we aim to uncover new insights into the nature of DM and its connection to the early Universe. Our study highlights the potential of inflationary GW observations as a powerful tool for investigating the properties of DM, offering a complementary approach to traditional collider and (in) direct-detection experiments.

II. THE DM RELIC DENSITY AND EARLY MATTER-DOMINATED ERA

In this work, we consider that the reheating temperature after inflation, T_R^I, is larger than the freeze-out temperature of light feebly interacting DM, T_f. Therefore, despite its feeble interactions with standard-model particles, light feebly interacting DM would freeze out in the early Universe due to the compensation of a high reheating temperature T_R^I. However, due to its feeble interaction, light feebly interacting DM decouples from the thermal bath in an early time, when the freeze-out temperature of light feebly interacting DM is still much higher than its rest mass, which provides the DM relic density as

$$\Omega_\chi h^2 = \frac{m_\chi Y_\infty s_0}{\rho_c} h^2 \approx 0.12 \left(\frac{m_\chi}{112\ \text{eV}}\right). \tag{1}$$

Here, $\Omega_\chi h^2$ represents the present-day DM relic density, m_χ is the DM mass, Y_∞ is the present-day DM yield, s_0 is the current entropy, ρ_c is the critical density, and h is the reduced Hubble constant. The DM yield is given by

$$Y_\infty = \frac{135\zeta(3)}{8\pi^4} \frac{g_\chi}{g_s(T_f)}, \tag{2}$$

where g_χ represents the internal degrees of freedom (d.o.f.'s) of DM, $g_s(T)$ is the effective number of relativistic d.o.f.'s of entropy at temperature T, and T_f is the freeze-out temperature of DM. In contrast to WIMP DM, the relic density of light feebly interacting DM can easily exceed the observed value of $\Omega_\chi^{\text{obs}} h^2 = 0.12$ due to its weaker annihilation cross section. To reconcile this discrepancy, the overproduced DM abundance can be diluted by extra entropy production, which is usually induced by a late-decaying state, resulting in an EMD era. It is important to note that the EMD scenario is merely one among various possibilities for explaining the observed relic density of dark matter. Additional mechanisms, including late-time entropy production from alternative sources or nonstandard interactions of dark matter, can also be taken into account. However, the key aspect that entropy dilution is correlated with the mass of dark matter remains independent of specific model details.

In this study, we consider the moduli as the late-decaying state [70]. The evolution of the early Universe during the EMD era is governed by the coupled Boltzmann equations,

$$\begin{aligned} \frac{d\phi_m}{dt} &= -\Gamma_m \phi_m, \\ \frac{d\phi_R}{dt} &= a\Gamma_m \phi_m, \end{aligned} \tag{3}$$

where ϕ_R and ϕ_m represent the comoving energy density of radiation and moduli, respectively. Γ_m is the decay width of moduli, a is the scale factor, and M_{Pl} is the reduced Planck mass. The Hubble expansion rate during the EMD era is given by

$$H^2 = \frac{1}{3M_{\text{Pl}}^2}\left(\frac{\phi_R}{a^4} + \frac{\phi_m}{a^3}\right). \tag{4}$$

The EMD era consists of adiabatic and nonadiabatic phases [29,30], starting at the cosmic temperature T_{eq} and ending at T_R. These characteristic temperatures, determined by the decay width and comoving energy density of the moduli, can be expressed as follows:

$$T_{\text{eq}} = \left(\frac{30\phi_m}{\pi^2 g_\rho(T_{\text{eq}})}\right)^{1/4}, \tag{5}$$

$$T_R = \left(\frac{90}{8\pi^3 g_\rho(T_R)}\right)^{1/4} \sqrt{\Gamma_m M_{\text{Pl}}}. \tag{6}$$

Here, $g_\rho(T)$ represents the effective number of relativistic d.o.f.'s of the energy density at the cosmic temperature T. The moduli decay injects additional entropy into the early Universe, and the resulting dilution effect can be parametrized by the dilution factor

$$D \equiv \frac{S_{\text{after}}}{S_{\text{before}}} = \frac{g_s(T_R)T_R^3}{g_s(T_{\text{eq}})T_{\text{eq}}^3} \frac{a(T_R)^3}{a(T_{\text{eq}})^3} = \frac{g_s(T_R)g_\rho(T_{\text{eq}})}{g_s(T_{\text{eq}})g_\rho(T_R)} \frac{T_{\text{eq}}}{T_R}, \tag{7}$$

where S_{before} (S_{after}) is the comoving entropy of the Universe before (after) moduli decay. We use the relation between the scalar factor and Hubble expansion rate in the EMD era, $a(T) \propto H(T)^{-2/3}$, to derive the dilution factor. It is worth noting that the dilution factor is valid for DM production before the beginning of the nonadiabatic EMD era. As the freeze-out temperature of light feebly

interacting DM is very high, the dilution from Eq. (7) is always valid in our scenario. The thermally overproduced DM abundance with different DM masses m_χ needs the suitable dilution factors $D = m_\chi/112$ to reconcile with the observations, where m_χ is in the units of eV. For example, the Lyman-α forest data sets put strong constraints on the free streaming of warm dark matter, further on the mass of a thermal relic warm dark matter, $m_\chi > 5.3$ keV [71], which implies that the dilution factor $D \approx 47$ at least is required to satisfy the warm dark matter thermal relic. The larger the DM mass m_χ is, the larger the required dilution factor is, as the thermally produced DM yield is proportional to m_χ. Besides, the entropy injection can not only dilute the DM thermal relic, but also cool down the DM velocity. The DM particle with mass m_χ that is thermal freeze-out when relativistic has a present-day velocity of

$$\langle v_\chi^0 \rangle \approx 0.023\ \mathrm{km\,s^{-1}} \left(\frac{g_\rho(T_f)}{100}\right)^{-1/3} \left(\frac{m}{1\ \mathrm{keV}}\right)^{-1}. \quad (8)$$

The limits between hot, warm, and cold dark matter are ambiguous. One can qualify as warm dark matter with velocity $0.0018\ \mathrm{km\,s^{-1}} \leq v_\chi^0 \leq 0.054\ \mathrm{km\,s^{-1}}$ [72]. The extra entropy injection after the DM thermal freeze-out cools down the DM velocity: $\langle v_\chi^0 \rangle \to \langle v_\chi^0 \rangle / D^{1/3}$. This indicates that the dilution factor $D \approx 72$ is required to satisfy warm dark matter bounds when $m_\chi = 0.1$ keV. Note that the dilution factor D relies on the two characteristic temperatures T_R and T_{eq}, which are related to the EMD era induced by the moduli. Intriguingly, the EMD era will cause two turning points in the primordial GW spectrum, whose frequencies are also dependent on these two characteristic temperatures. This indicates that the primordial GW spectrum can be utilized to look for light feebly interacting DM. In the next section, we will evaluate the primordial GW spectrum during an EMD era and discuss the prospect of DM detection through primordial GWs.

III. THE PRIMORDIAL GRAVITATIONAL WAVE SPECTRUM IN THE EMD ERA

Primordial gravitational waves represent tensor perturbations in a spatially flat Friedmann-Robertson-Walker (FRW) universe, described by the metric

$$ds^2 = -dt^2 + a^2(t)(\delta_{ij} + h_{ij}(t, \vec{x}))dx^i dx^j. \quad (9)$$

Here, the gauge-invariant tensor perturbation h_{ij} satisfies $h_{ij} = h_{ji}$, along with the transverse and traceless conditions: $h_{ii} = 0$ and $h_{ij,j} = 0$. By treating h_{ij} as a quantum field, we obtain the equation of motion for freely propagating GWs without the anisotropic stress of the energy-momentum tensor ($\Pi_{ij} = 0$). Thus, the equations of motion for the tensor modes $h_k(\tau)$ in Fourier space are described by

$$\left[\frac{d^2}{d\tau^2} + \frac{2}{a}\frac{da}{d\tau}\frac{d}{d\tau} + k^2\right] h_k(\tau) = 0, \quad (10)$$

where k is the wave number, and τ represents the conformal time with its derivative $d\tau = dt/a$. The current energy spectrum of primordial GWs is given by the present-day tensor power spectrum $\Delta_h^2(k, \tau_0)$:

$$\Omega_0^{\mathrm{GW}}(f) = \frac{1}{12}\left(\frac{2\pi f}{H_0}\right)^2 \Delta_h^2(k, \tau_0), \qquad f = \frac{k}{2\pi a_0}. \quad (11)$$

The wave numbers k are outside the horizon during inflation, implying that the tensor modes $h_k(\tau)$ are independent of the conformal time τ until the wave numbers k reenter the horizon. Consequently, the present-day tensor power spectrum is related to the primordial tensor power spectrum through the tensor transfer function $T_h(k)$ [58]:

$$\Delta_h^2(k, \tau_0) = T_h(k)\Delta_h^2(k, \tau_i). \quad (12)$$

The transfer function behaves as $T_h(k) \sim (a_k^2/a_0^2)$ [52–54], where $a_k = k/H(a_k)$ is the scale factor at the k-mode horizon reentry and depends on the equation of state (EOS) at the time of horizon reentry. More details about the tensor transfer function can be found in Ref. [58]. The calculations of the primordial tensor power spectrum are conventionally based on the CMB pivot wave number k_{cmb}. Eventually, the current energy spectrum $\Omega_0^{\mathrm{GW}}(f)$ is described by the primordial tensor amplitude A_t,

$$\Omega_0^{\mathrm{GW}}(f) = \frac{1}{12} T_h(k)\left(\frac{2\pi f}{H_0}\right)^2 A_t \left(\frac{k}{k_{\mathrm{cmb}}}\right)^{n_t}, \quad (13)$$

where n_t is the tensor spectral index. The primordial GW signals are strongly enhanced by both primordial tensor amplitude A_t and tensor spectral index n_t. We therefore reasonably set the maximum A_t and n_t so that the present-day and future GW detectors can detect the primordial GW signals as much as possible. The maximum A_t depends on the amplitude of the primordial scalar spectrum A_s and the tensor-to-scalar ratio $r = A_t/A_s \lesssim 0.07$ [73]. According to the measured primordial scalar spectrum $A_s = 2.1 \times 10^{-9}$, the maximally allowed A_t is set to 1.5×10^{-10}. On the other hand, we take the similar maximum $n_t = 0.4$ as discussed in Ref. [69]. Besides this, the primordial GW power spectrum decreases with the increase of r. Therefore, we investigate the primordial GW power spectrum without an EMD era by fixing $r = 0.07$ for detectability. We find that the GW primordial spectrum generated by $n_t < 0.13$ is beyond the range of the cosmic explorer (CE) [74] detector, while that produced by $n_t < -0.1$ is beyond the detection capability of the big bang observer (BBO) [75–77] detector.

The EMD era leaves distinct imprints on the primordial GW spectrum, where two characteristic features can be identified—the EMD bump and the matter-dominated tail:

(i) *EMD bump:* During the EMD era, the background expansion of the Universe transitions from an accelerated phase to a decelerated phase. This changes the tensor transfer function from $T_h(k) \propto f^{-2}$ to $T_h(k) \propto f^{-4}$, resulting in one kink and a temporary enhancement in the primordial GW spectrum at certain frequencies. This feature is known as the EMD bump. The EMD bump arises due to the presence of additional sources of anisotropic stress during the EMD era, such as collisionless particles or cosmic defects. The amplitude and shape of the EMD bump depend on the properties of these additional sources. The EMD bump is typically characterized by its peak frequency $f_{\rm peak}$ and its amplitude relative to the inflationary background.

(ii) *Matter-dominated tail:* After the EMD era, the Universe enters the regular radiation-dominated era, during which the primordial GW spectrum continues to evolve. The tensor transfer function evolves from $T_h(k) \propto f^{-4}$ to $T_h(k) \propto f^{-2}$, leading to another kink in the primordial GW spectrum at certain frequency. Also, the amplitude of the primordial GW spectrum decreases as $\Omega^{\rm GW}(f) \propto f^{n_t}$ for frequencies below the peak frequency $f_{\rm peak}$. This power-law behavior is known as the matter-dominated tail of the primordial GW spectrum. The matter-dominated tail extends to lower frequencies and provides a unique signature of the early Universe dynamics.

The detection and characterization of the EMD bump and the matter-dominated tail in the primordial GW spectrum can provide valuable insights into the physics of the early Universe, including the nature of the EMD era and the generation mechanisms of primordial GWs. The EMD bump and matter-dominated tail occur at the two characteristic temperatures $T_{\rm eq}$ and T_R, respectively, which single out two corresponding frequencies $f(T_{\rm eq})$ and $f(T_R)$. The frequency $f(T_R)$ at temperature T_R can be obtained by Eq. (11):

$$f(T_R) = \frac{a(T_R)H(T_R)}{a_0 H_0} f(T_0) = \left(\frac{g_s(T_0)}{g_s(T_R)}\right)^{1/3} \left(\frac{g_\rho(T_R)}{g_\rho(T_0)}\right)^{1/2} (2\Omega_R^0)^{1/2} \frac{T_R}{T_0} f(T_0), \tag{14}$$

where $T_0 = 2.72548$ K [78] is the present temperature of the cosmic microwave background (CMB) and $f(T_0) = H_0/2\pi$ denotes the current frequency of the GW mode. $H_0 = 100h$ km/s/Mpc is the present-day Hubble expansion rate, and Ω_R^0 represents the ratio of the current radiation energy density and critical density. Likewise, we can derive the frequency $f(T_{\rm eq})$ by exploiting the relationship between temperature and frequency:

$$f(T_{\rm eq}) = \left(\frac{g_\rho(T_R)}{g_\rho(T_{\rm eq})}\right)^{-1/6} \left(\frac{T_{\rm eq}}{T_R}\right)^{2/3} f(T_R). \tag{15}$$

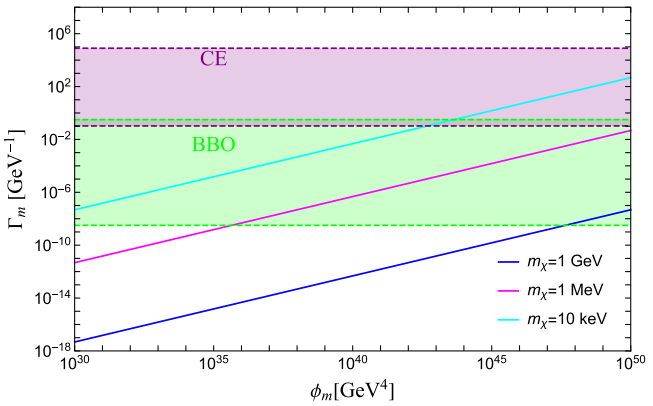

FIG. 1. The contour plots of observed DM relic density with different masses m_χ as a function of decay width Γ_m and the comoving energy density ϕ_m. The blue, magenta, and cyan contour plots are for $m_\chi = 10$ keV, $m_\chi = 1$ MeV, and $m_\chi = 1$ GeV, respectively. The purple (green) shaded region indicates the case where the lower kink frequency $f(T_R)$ is within the sensitivity of the CE (BBO) detector.

In Eqs. (5) and (6), these two characteristic temperatures T_R and $T_{\rm eq}$ are only functions of the decay width Γ_m and the comoving energy density ϕ_m, respectively, which ensures that the frequency $f(T_R)$ is a function of Γ_m only while $f(T_{\rm eq})$ is a function of both Γ_m and ϕ_m. Hence, we first study the case where the lower frequency $f(T_R)$ is detected by GW detectors such as the CE and BBO, as it is only connected with Γ_m. In Fig. 1, we show, by the shaded region, the parameter space that leads to the lower kink frequency $f(T_R)$ that can be covered by BBO or CE GW experiments. The parameter regions that can provide observed DM relic density for different choices of DM mass are also indicated by the solid lines with different colors. More importantly, the behavior of the transfer function $T_h(k)$ is modified by the EMD era, which eventually leads to a change in the spectral index of the GW spectrum:

$$n = n_t + 2 \times \frac{3\omega - 1}{3\omega + 1}, \tag{16}$$

where $\omega = 0$ arises from the EOS during an EMD era.[1] Therefore, the spectra index of the GW spectrum changes by

[1]It should be noted that the nonstandard cosmological models with EOS $\omega = 0$ will leave similar signatures on the gravitational spectrum compared to the EMD era. This indicates that the EMD era may be difficult to distinguish from the phase transition or more complex inflationary dynamics in this scenario.

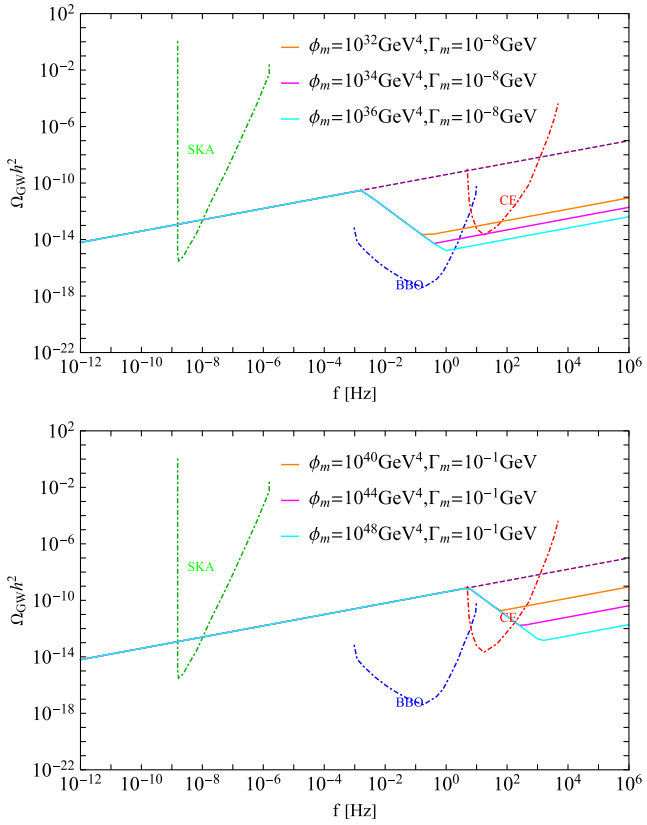

FIG. 2. The present-day primordial GWs spectra $\Omega_{GW}h^2$ as a function of the frequency. In both the upper and lower panels, the solid lines illustrate the primordial GW spectra within the EMD era induced by different relevant parameters, while the purple dashed line represents that without the EMD era. The dot-dashed lines show the sensitivity of various GW detectors, such as SKA [79–81], BBO [75–77], and CE [74]. The upper (lower) panel shows that the primordial GW spectra lie within the sensitivity of BBO (CE).

$\delta n = -2$ during an EMD era. This implies that the GW spectrum drops sharply within the EMD era and has a steplike feature between the frequencies $f(T_R)$ and $f(T_{\rm eq})$. The GW energy density values, which are also diluted by the entropy produced during the EMD era, at the frequencies of these two kinks are approximately related to the dilution factor by [69]

$$\frac{\Omega^0_{GW}(f(T_{\rm eq}))}{\Omega^0_{GW}(f(T_R))} \approx \left(\frac{f(T_{\rm eq})}{f(T_R)}\right)^{n_t} D^{-4/3}. \tag{17}$$

As mentioned before, the thermally produced DM relic density with a larger mass requires a larger dilution factor from the EMD era to reconcile with the observations. On the other hand, the EMD era also imprints unique features in the GW spectra. Therefore, probing the light feebly interacting DM and the measurement of the GW spectrum are strongly correlated. In Fig. 2, we show the primordial GW spectra for different parameters that are within the sensitivity of BBO (blue dashed line) and CE (red dashed line) experiments. The kinks of the primordial GW spectrum imply the onset and end of the EMD era. Furthermore, one can infer the EOS $\omega = p/\rho$ during the early Universe according to the slopes of the kinks. As the lower kink frequency $f(T_R)$ only relies on the decay width of moduli Γ_m, the locations of kinks at lower frequencies are the same for the same decay width Γ_m. However, the higher kink frequency $f(T_{\rm eq})$ and dilution factor D are related to both the comoving energy density ϕ_m and the decay width Γ_m of moduli. Additionally, they both increase with the comoving energy density of moduli ϕ_m increasing. Consequently, the GW spectrum has strong dilution behavior, which is correlated with the light feebly interacting DM mass through the observed relic density. Provided that the GW spectrum can be exactly observed by GW detectors, the light feebly interacting DM mass m_χ can also be accurately predicted in this scenario. Besides this, the light feebly interacting DM and standard model particles in the general EMD era models can be simultaneously produced by the long-lived parent particle decay at a collider. The long-lived parent particle decay leads to various displaced collider signals such as displaced vertices, displaced jets/leptons, and stopped particle decays. Therefore, one can also infer the DM mass from displaced signatures at the collider [20].

A. Benchmark model: Supersymmetry DFSZ axion model

In the SUSY DFSZ axion model, the axino, the fermionic superpartner of the axion, is a natural light feebly interacting dark matter candidate. The axino would freeze out at the cosmic temperature

$$T^f_{\tilde a} \approx 10^{10}\ {\rm GeV}\left(\frac{V_{\rm PQ}}{10^{12}\ {\rm GeV}}\right)^2\left(\frac{1}{\alpha_s}\right)^3, \tag{18}$$

where $V_{\rm PQ}$ is the PQ symmetry breaking scale, and α_s is the strong interaction coupling constant. When the reheating temperature T^I_R after inflation is larger than the axino freeze-out temperature $T^f_{\tilde a}$, the axino will be in thermal equilibrium, and its thermal produced relic abundance is

$$\Omega_\chi h^2 = \frac{m_{\tilde a} Y_{\tilde a} s_0}{\rho_c} h^2, \tag{19}$$

with the axino yield

$$Y_{\tilde a} = \frac{135\zeta(3) g_{\tilde a}}{8\pi^4 g_s(T^f_{\tilde a})}, \tag{20}$$

where $g_{\tilde a} = 2$ is the internal d.o.f. of the axino. The axino abundance produced by thermal freeze-out will easily overclose the Universe. Fortunately, there exists the saxion (the real part of the axion field) in the SUSY DFSZ model. The supersymmetry breaking provides the saxion field with

a large potential $\rho_s = m_s^2 s_I^2$ after inflation, which leads to the EMD era in the Universe. The onset and end of the EMD era induced by the saxion correspond to the cosmological temperatures T_M and T_{Rs}:

$$T_M = 3\left(\frac{10}{g_\rho(T_M)\pi^2}\right)^{1/4} \frac{m_s^{1/2} s_I^2}{M_{\rm Pl}^{3/2}}, \tag{21}$$

$$T_{Rs} = \left(\frac{90}{\pi^2 g_\rho(T_{Rs})}\right)^{1/4} \sqrt{\Gamma_s M_{\rm Pl}}, \tag{22}$$

where m_s and Γ_s are the mass and decay width of the saxion, respectively. The EMD era will result in two kinks on the primordial GW spectrum, corresponding to the characteristic frequencies $f(T_M)$ and $f(T_{Rs})$:

$$f(T_{Rs}) = \left(\frac{g_s(T_0)}{g_s(T_{Rs})}\right)^{1/3} \left(\frac{g_\rho(T_{Rs})}{g_\rho(T_0)}\right)^{1/2} (2\Omega_R^0)^{1/2} \frac{T_{Rs}}{T_0} f(T_0), \tag{23}$$

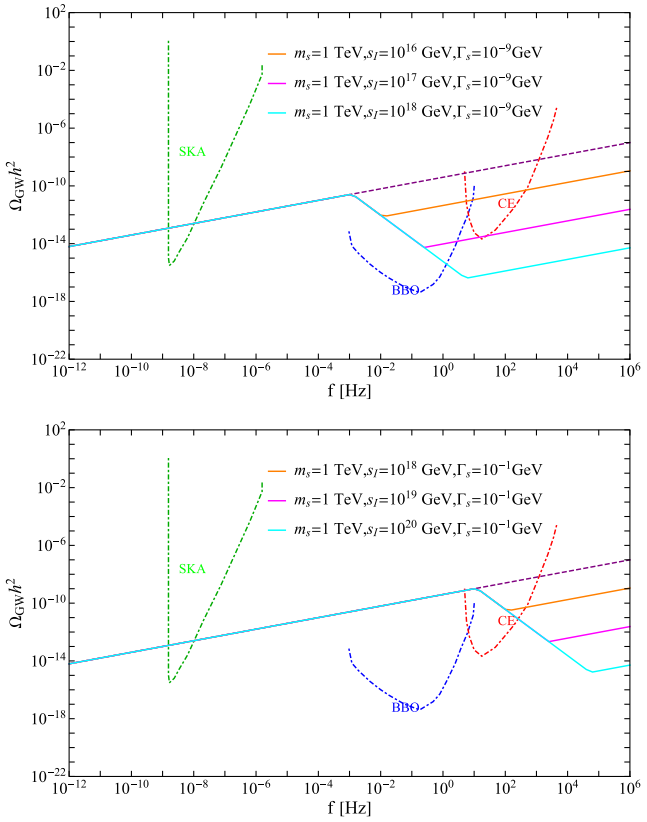

FIG. 3. The present-day primordial GWs spectra $\Omega_{\rm GW}h^2$ in the SUSY DFSZ axion model as a function of the frequency. These parameters related to the saxion are shown. In both the upper and lower panels, the solid lines illustrate the primordial GW spectra within the EMD era induced by different relevant parameters, while the purple dashed line represents that without the EMD era.

$$f(T_M) = \left(\frac{g_\rho(T_{Rs})}{g_\rho(T_M}\right)^{-1/6} \left(\frac{T_M}{T_{Rs}}\right)^{2/3} f(T_{Rs}). \tag{24}$$

After the end of the EMD era, an amount of entropy is injected into the Universe and dilutes the overproduced axino relic. The dilution effect can be described by the dilution factor,

$$D_s = \left(\frac{9 g_\rho(T_{Rs})}{g_\rho(T_M)}\right)^{1/4} \frac{m_s^{1/2} s_I^2}{\sqrt{\Gamma_s} M_{\rm Pl}^2}. \tag{25}$$

With these in hand, we can calculate the primordial GW spectrum in the SUSY DFSZ axion model, as shown in Fig. 3. If these two kinks on the primordial GW spectrum are fully detected by BBO or CE detectors, we can infer the parameters related to the saxion according to the primordial GW spectrum. For example, if the magenta line is observed by the BBO detector, we can evaluate $\Gamma_s = 10^{-9}$ GeV and $s_I = 10^{17}$ GeV for a fixed saxion mass $m_s = 1$ TeV. Under these parameters, the dilution factor $D \approx 1360$ and the axino mass $m_{\tilde{a}} \approx 326$ keV are determined by the dilution factor according to the observed DM abundance.

IV. CONCLUSIONS

The exploration of light feebly interacting DM is challenging through traditional DM direct-detection experiments due to its feeble interactions. However, gravitational waves (GWs) offer a novel and complementary avenue for probing the early Universe and searching for light feebly interacting DM. This approach can be utilized in conjunction with collider experiments and indirect/direct detections. In particular, the entropy production period plays a crucial role in addressing the overabundance of thermally produced light feebly interacting DM relic density. On the other hand, such an entropy production period also leaves imprints on the primordial GW spectrum, giving rise to distinct features characterized by two kinks with the frequencies corresponding to the starting ($T_{\rm eq}$) and ending (T_R) temperatures of the entropy production period. This is illustrated in our work by an EMD era induced by the moduli.

The detection and characterization of these modified GW spectra within the sensitivities of GW detectors such as BBO and CE provide a unique opportunity to probe the existence of light feebly interacting DM. The DM masses m_χ can be further inferred under the same set of parameters. Moreover, with the continuous improvement in precision, range, and sensitivity of GW detectors, as well as the synergistic combination of different GW experiments, the primordial GW spectrum can be measured more accurately and extensively. Consequently, probing light feebly interacting DM through the GW spectrum becomes a highly promising avenue in the foreseeable future.

ACKNOWLEDGMENTS

L. W. is supported by the National Natural Science Foundation of China (NNSFC) under Grants No. 12335005, No. 12275134, and No. 12147228. B. Z. is supported by NNSFC under Grants No. 12275232 and No. 11835005. Y. W. is supported by NNSFC under Grant No. 12305112 and also would like to thank Nanjing Normal University for its support.

[1] E. Aprile *et al.* (XENON Collaboration), Constraining the spin-dependent WIMP-nucleon cross sections with XENON1T, Phys. Rev. Lett. **122**, 141301 (2019).
[2] Z. Z. Liu *et al.* (CDEX Collaboration), Constraints on spin-independent nucleus scattering with sub-GeV weakly interacting massive particle dark matter from the CDEX-1B experiment at the China Jinping Underground Laboratory, Phys. Rev. Lett. **123**, 161301 (2019).
[3] C. Fu *et al.* (PandaX-II Collaboration), Spin-dependent weakly-interacting-massive-particle–nucleon cross section limits from first data of PandaX-II experiment, Phys. Rev. Lett. **118**, 071301 (2017); **120**, 049902(E) (2018).
[4] J. Aalbers *et al.* (LUX-ZEPLIN Collaboration), First dark matter search results from the LUX-ZEPLIN (LZ) experiment, Phys. Rev. Lett. **131**, 041002 (2023).
[5] D. S. Akerib *et al.* (LUX Collaboration), Results from a search for dark matter in the complete LUX exposure, Phys. Rev. Lett. **118**, 021303 (2017).
[6] K. Choi *et al.* (Super-Kamiokande Collaboration), Search for neutrinos from annihilation of captured low-mass dark matter particles in the Sun by Super-Kamiokande, Phys. Rev. Lett. **114**, 141301 (2015).
[7] M. Ackermann *et al.* (Fermi-LAT Collaboration), The spectrum of isotropic diffuse gamma-ray emission between 100 MeV and 820 GeV, Astrophys. J. **799**, 86 (2015).
[8] M.-Y. Cui, Q. Yuan, Y.-L. S. Tsai, and Y.-Z. Fan, Possible dark matter annihilation signal in the AMS-02 antiproton data, Phys. Rev. Lett. **118**, 191101 (2017).
[9] A. M. Sirunyan *et al.* (CMS Collaboration), Search for new physics in final states with a single photon and missing transverse momentum in proton-proton collisions at $\sqrt{s} = 13$ TeV, J. High Energy Phys. 02 (2019) 074.
[10] L. Su, W. Wang, L. Wu, J. M. Yang, and B. Zhu, Atmospheric Dark Matter and Xenon1T Excess, Phys. Rev. D **102**, 115028 (2020).
[11] P. Athron *et al.*, Global fits of axion-like particles to XENON1T and astrophysical data, J. High Energy Phys. 05 (2021) 159.
[12] G. H. Duan, X.-G. He, L. Wu, and J. M. Yang, Leptophilic dark matter in gauged $U(1)_{L_e-L_\mu}$ model in light of DAMPE cosmic ray $e^+ + e^-$ excess, Eur. Phys. J. C 78, 323 (2018).
[13] G. Arcadi, M. Dutra, P. Ghosh, M. Lindner, Y. Mambrini, M. Pierre, S. Profumo, and F. S. Queiroz, The waning of the WIMP? A review of models, searches, and constraints, Eur. Phys. J. C **78**, 203 (2018).
[14] E. Aprile *et al.* (XENON Collaboration), Dark matter search results from a one ton-year exposure of XENON1T, Phys. Rev. Lett. **121**, 111302 (2018).
[15] T. Moroi, H. Murayama, and M. Yamaguchi, Cosmological constraints on the light stable gravitino, Phys. Lett. B **303**, 289 (1993).
[16] L. Covi, J. E. Kim, and L. Roszkowski, Axinos as cold dark matter, Phys. Rev. Lett. **82**, 4180 (1999).
[17] L. Covi, H.-B. Kim, J. E. Kim, and L. Roszkowski, Axinos as dark matter, J. High Energy Phys. 05 (2001) 033.
[18] L. Roszkowski, R. Ruiz de Austri, and K.-Y. Choi, Gravitino dark matter in the CMSSM and implications for leptogenesis and the LHC, J. High Energy Phys. 08 (2005) 080.
[19] K. J. Bae, H. Baer, E. J. Chun, and C. S. Shin, Mixed axion/gravitino dark matter from SUSY models with heavy axinos, Phys. Rev. D **91**, 075011 (2015).
[20] R. T. Co, F. D'Eramo, L. J. Hall, and D. Pappadopulo, Freeze-in dark matter with displaced signatures at colliders, J. Cosmol. Astropart. Phys. 12 (2015) 024.
[21] A. Brandenburg, L. Covi, K. Hamaguchi, L. Roszkowski, and F. D. Steffen, Signatures of axinos and gravitinos at colliders, Phys. Lett. B **617**, 99 (2005).
[22] K.-Y. Choi, D. Restrepo, C. E. Yaguna, and O. Zapata, Indirect detection of gravitino dark matter including its three-body decays, J. Cosmol. Astropart. Phys. 10 (2010) 033.
[23] G. A. Gómez-Vargas, D. E. López-Fogliani, C. Muñoz, and A. D. Perez, MeV-GeV γ-ray telescopes probing axino LSP/gravitino NLSP as dark matter in the $\mu\nu$SSM, J. Cosmol. Astropart. Phys. 01 (2020) 058.
[24] G. A. Gómez-Vargas, D. E. López-Fogliani, C. Muñoz, and A. D. Perez, MeV-GeV γ-ray telescopes probing gravitino LSP with coexisting axino NLSP as dark matter in the $\mu\nu$ SSM, Astropart. Phys. **125**, 102506 (2021).
[25] Y. Gu, L. Wu, and B. Zhu, Axion dark radiation: Hubble tension and the Hyper-Kamiokande neutrino experiment, Phys. Rev. D **105**, 095008 (2022).
[26] M. Bolz, A. Brandenburg, and W. Buchmuller, Thermal production of gravitinos, Nucl. Phys. **B606**, 518 (2001); **B790**, 336(E) (2008).
[27] J. Pradler and F. D. Steffen, Thermal gravitino production and collider tests of leptogenesis, Phys. Rev. D **75**, 023509 (2007).
[28] J. Pradler and F. D. Steffen, Constraints on the reheating temperature in gravitino dark matter scenarios, Phys. Lett. B **648**, 224 (2007).
[29] R. T. Co, F. D'Eramo, and L. J. Hall, Gravitino or axino dark matter with reheat temperature as high as 10^{16} GeV, J. High Energy Phys. 03 (2017) 005.
[30] R. T. Co, F. D'Eramo, L. J. Hall, and K. Harigaya, Saxion cosmology for thermalized gravitino dark matter, J. High Energy Phys. 07 (2017) 125.

[31] T. Asaka, K. Hamaguchi, and K. Suzuki, Cosmological gravitino problem in gauge mediated supersymmetry breaking models, Phys. Lett. B **490**, 136 (2000).
[32] C. Cheung, G. Elor, and L. J. Hall, The cosmological axino problem, Phys. Rev. D **85**, 015008 (2012).
[33] T. Moroi and L. Randall, Wino cold dark matter from anomaly mediated SUSY breaking, Nucl. Phys. **B570**, 455 (2000).
[34] S. D. Thomas, Baryons and dark matter from the late decay of a supersymmetric condensate, Phys. Lett. B **356**, 256 (1995).
[35] T. Moroi, M. Yamaguchi, and T. Yanagida, On the solution to the Polonyi problem with 0 (10-TeV) gravitino mass in supergravity, Phys. Lett. B **342**, 105 (1995).
[36] R. Allahverdi and M. Drees, Production of massive stable particles in inflaton decay, Phys. Rev. Lett. **89**, 091302 (2002).
[37] T. Moroi and T. Takahashi, Cosmic density perturbations from late decaying scalar condensations, Phys. Rev. D **66**, 063501 (2002).
[38] A. B. Lahanas, Dilaton dominance in the early Universe dilutes dark matter relic abundances, Phys. Rev. D **83**, 103523 (2011).
[39] M. Fujii and K. Hamaguchi, Nonthermal dark matter via Affleck-Dine baryogenesis and its detection possibility, Phys. Rev. D **66**, 083501 (2002).
[40] C. Cosme, M. Dutra, T. Ma, Y. Wu, and L. Yang, Neutrino portal to FIMP dark matter with an early matter era, J. High Energy Phys. 03 (2021) 026.
[41] Y. Gu, M. Khlopov, L. Wu, J. M. Yang, and B. Zhu, Light gravitino dark matter: LHC searches and the Hubble tension, Phys. Rev. D **102**, 115005 (2020).
[42] M. Nemevšek and Y. Zhang, Dark matter dilution mechanism through the lens of large-scale structure, Phys. Rev. Lett. **130**, 121002 (2023).
[43] J. Aasi *et al.* (LIGO Scientific Collaboration), Advanced LIGO, Classical Quantum Gravity **32**, 074001 (2015).
[44] F. Acernese *et al.* (Virgo Collaboration), Advanced Virgo: A second-generation interferometric gravitational wave detector, Classical Quantum Gravity **32**, 024001 (2015).
[45] B. P. Abbott *et al.* (LIGO Scientific and Virgo Collaborations), Observation of gravitational waves from a binary black hole merger, Phys. Rev. Lett. **116**, 061102 (2016).
[46] H. B. Nielsen and P. Olesen, Vortex line models for dual strings, Nucl. Phys. **B61**, 45 (1973).
[47] T. W. B. Kibble, Topology of cosmic domains and strings, J. Phys. A **9**, 1387 (1976).
[48] M. B. Hindmarsh and T. W. B. Kibble, Cosmic strings, Rep. Prog. Phys. **58**, 477 (1995).
[49] L. F. Abbott and M. B. Wise, Constraints on generalized inflationary cosmologies, Nucl. Phys. **B244**, 541 (1984).
[50] D. J. Weir, Gravitational waves from a first order electroweak phase transition: A brief review, Phil. Trans. R. Soc. A **376**, 20170126 (2018).
[51] P. Athron, C. Balázs, A. Fowlie, L. Morris, and L. Wu, Cosmological phase transitions: From perturbative particle physics to gravitational waves, Prog. Part. Nucl. Phys. **135**, 104094 (2024).
[52] M. S. Turner, M. J. White, and J. E. Lidsey, Tensor perturbations in inflationary models as a probe of cosmology, Phys. Rev. D **48**, 4613 (1993).
[53] L. A. Boyle and P. J. Steinhardt, Probing the early Universe with inflationary gravitational waves, Phys. Rev. D **77**, 063504 (2008).
[54] Y. Watanabe and E. Komatsu, Improved calculation of the primordial gravitational wave spectrum in the standard model, Phys. Rev. D **73**, 123515 (2006).
[55] S. Kuroyanagi, K. Nakayama, and S. Saito, Prospects for determination of thermal history after inflation with future gravitational wave detectors, Phys. Rev. D **84**, 123513 (2011).
[56] S. Kuroyanagi, T. Chiba, and T. Takahashi, Probing the Universe through the stochastic gravitational wave background, J. Cosmol. Astropart. Phys. 11 (2018) 038.
[57] N. Bernal and F. Hajkarim, Primordial gravitational waves in nonstandard cosmologies, Phys. Rev. D **100**, 063502 (2019).
[58] L. A. Boyle and A. Buonanno, Relating gravitational wave constraints from primordial nucleosynthesis, pulsar timing, laser interferometers, and the CMB: Implications for the early Universe, Phys. Rev. D **78**, 043531 (2008).
[59] Y. Cui, M. Lewicki, D. E. Morrissey, and J. D. Wells, Cosmic archaeology with gravitational waves from cosmic strings, Phys. Rev. D **97**, 123505 (2018).
[60] C. Caprini and D. G. Figueroa, Cosmological backgrounds of gravitational waves, Classical Quantum Gravity **35**, 163001 (2018).
[61] Y. Cui, M. Lewicki, D. E. Morrissey, and J. D. Wells, Probing the pre-BBN universe with gravitational waves from cosmic strings, J. High Energy Phys. 01 (2019) 081.
[62] G. Bertone *et al.*, Gravitational wave probes of dark matter: Challenges and opportunities, SciPost Phys. Core **3**, 007 (2020).
[63] C. Yuan, R. Brito, and V. Cardoso, Probing ultralight dark matter with future ground-based gravitational-wave detectors, Phys. Rev. D **104**, 044011 (2021).
[64] L. Tsukada, R. Brito, W. E. East, and N. Siemonsen, Modeling and searching for a stochastic gravitational-wave background from ultralight vector bosons, Phys. Rev. D **103**, 083005 (2021).
[65] A. Chatrchyan and J. Jaeckel, Gravitational waves from the fragmentation of axion-like particle dark matter, J. Cosmol. Astropart. Phys. 02 (2021) 003.
[66] R. Samanta and F. R. Urban, Testing super heavy dark matter from primordial black holes with gravitational waves, J. Cosmol. Astropart. Phys. 06 (2022) 017.
[67] D. Borah, S. Jyoti Das, A. K. Saha, and R. Samanta, Probing WIMP dark matter via gravitational waves' spectral shapes, Phys. Rev. D **106**, L011701 (2022).
[68] Y. Gouttenoire, G. Servant, and P. Simakachorn, Beyond the standard models with cosmic strings, J. Cosmol. Astropart. Phys. 07 (2020) 032,
[69] F. D'Eramo and K. Schmitz, Imprint of a scalar era on the primordial spectrum of gravitational waves, Phys. Rev. Res. **1**, 013010 (2019).
[70] J. A. Evans, A. Ghalsasi, S. Gori, M. Tammaro, and J. Zupan, Light dark matter from entropy dilution, J. High Energy Phys. 02 (2020) 151.

[71] V. Iršič *et al.*, New Constraints on the free-streaming of warm dark matter from intermediate and small scale Lyman-α forest data, Phys. Rev. D **96**, 023522 (2017).
[72] K. Jedamzik, M. Lemoine, and G. Moultaka, Gravitino dark matter in gauge mediated supersymmetry breaking, Phys. Rev. D **73**, 043514 (2006).
[73] Y. Akrami *et al.* (Planck Collaboration), Planck 2018 results: X. Constraints on inflation, Astron. Astrophys. **641**, A10 (2020).
[74] B. P. Abbott *et al.* (LIGO Scientific Collaboration), Exploring the sensitivity of next generation gravitational wave detectors, Classical Quantum Gravity **34**, 044001 (2017).
[75] J. Crowder and N. J. Cornish, Beyond LISA: Exploring future gravitational wave missions, Phys. Rev. D **72**, 083005 (2005).
[76] V. Corbin and N. J. Cornish, Detecting the cosmic gravitational wave background with the big bang observer, Classical Quantum Gravity **23**, 2435 (2006).
[77] K. Yagi and N. Seto, Detector configuration of DECIGO/BBO and identification of cosmological neutron-star binaries, Phys. Rev. D **83**, 044011 (2011); **95**, 109901(E) (2017).
[78] D. J. Fixsen, The temperature of the cosmic microwave background, Astrophys. J. **707**, 916 (2009).
[79] C. L. Carilli and S. Rawlings, Science with the square kilometer array: Motivation, key science projects, standards and assumptions, New Astron. Rev. **48**, 979 (2004).
[80] G. Janssen *et al.*, Gravitational wave astronomy with the SKA, Proc. Sci. AASKA14 (**2015**) 037 [arXiv:1501.00127].
[81] A. Weltman *et al.*, Fundamental physics with the square kilometre array, Pub. Astron. Soc. Aust. **37**, e002 (2020).